Chapter 2

The Detector

Near Geneva (Switzerland) is situated one of the world largest accelerator centres: CERN. Several accelerators were built here, the largest of which is the Large Electron Positron collider LEP. It was decided that LEP would operate in two phases. In the first phase (LEP-I) it accelerated electrons and positrons up to about 46 GeV in opposite direction, providing the centre-of-mass energies needed to cover the Z resonance region. During the LEP-I phase the Standard Model parameters connected to the Z boson were measured with high accuracy. In the second phase (LEP-II) it accelerates electrons and positrons up to about 100 GeV, providing a centre-of-mass energy of about 200 GeV. During the LEP-II phase measurements are being performed at the W pair production and a possibility exists to discover the Higgs particle.

LEP is installed in a 26.7 km long tunnel down to about 100 m under the surface near the French-Swiss border. It consists of eight straight sections and eight curved ones. Four of the straight sections are housing large particle detectors: ALEPH, OPAL, DELPHI and L3, of which the L3 detector is the one used for this analysis. This detector is briefly described in the next section with the exception of the Silicon Micro-vertex Detector (SMD), which is described in greater detail in section 2.2. The simulation of the behaviour of particles in the L3 detector is briefly described in section 2.3.

2.1 The L3 detector

In figure 2.2 a perspective view of the L3 detector is shown. The origin, i.e., the point where the particles collide, is at the centre of the detector. The x-axis is towards the centre of the LEP ring, the y-axis is directed upwards and the z-axis is directed parallel to the beam pipe pointing in the direction of flight of the electron beam. In this analysis often the spherical coordinates r, θ, ϕ, will be used, were r is the distance to the centre of the detector, θ the angle between the z-axis and the $\vec{r}$ vector and ϕ the angle between the x-axis and the projection $\vec{s}$ of $\vec{r}$ on the xy-plane.

The L3 detector consists of several subdetectors each having its special characteristics and particular purpose. The whole detector is placed inside a large ($12 \times 12 \times 12$ m^3) magnet which provides a uniform magnetic field of 0.5 T.

The innermost part of the detector takes care of the tracking of charged particles. It is also

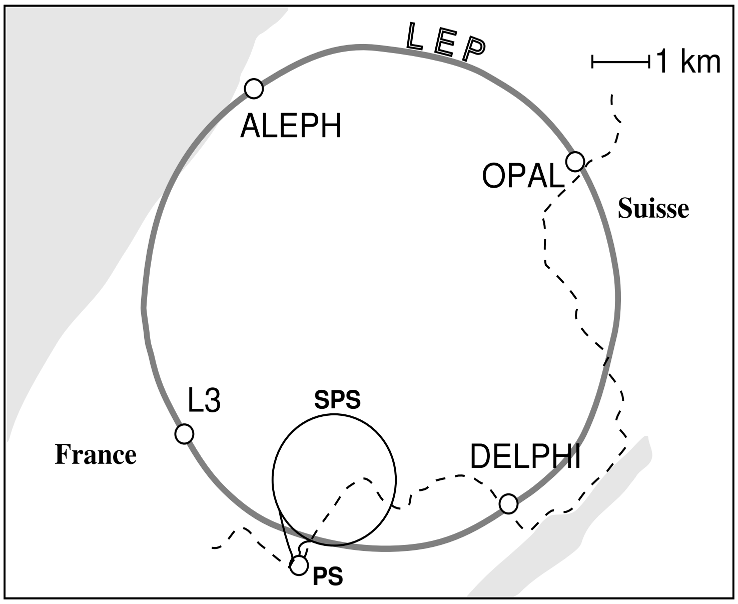

Figure 2.1: *The* LEP *ring.*

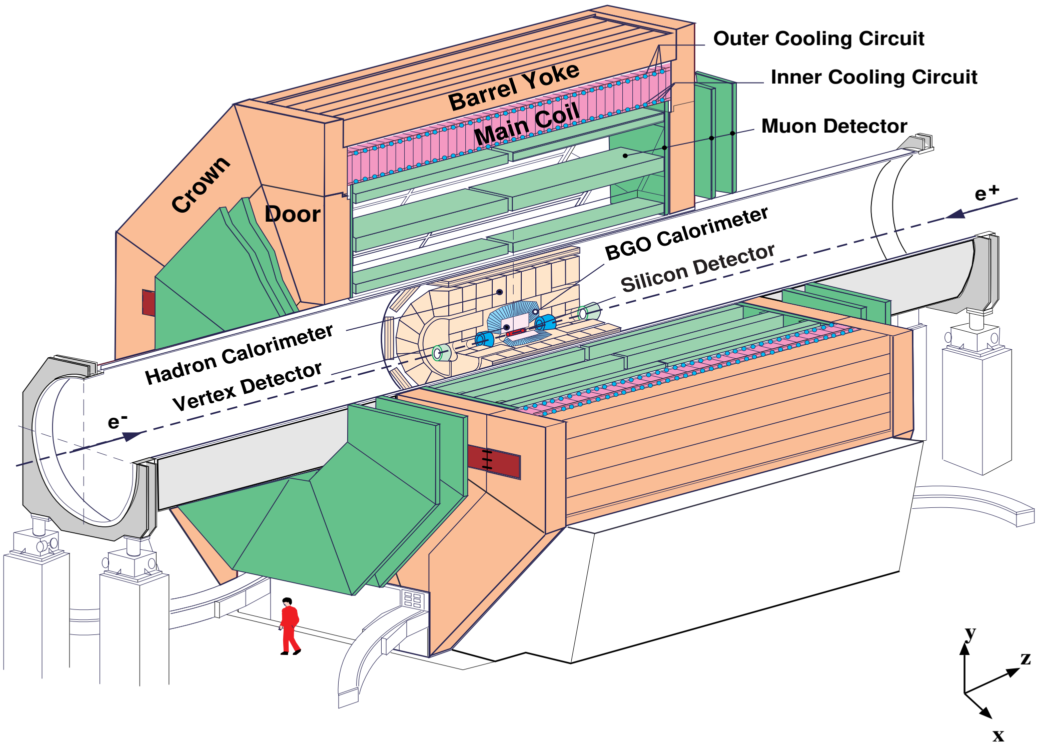

Figure 2.2: *A schematic view of the* L3 *detector.*

used to reconstruct the primary e^+e^- interaction point and possible decay (i.e. secondary) vertices of (long) lived particles, such as the B meson. It consists of :

- A Time Expansion wire Chamber (TEC) to measure the direction and curvature (i.e. the momentum) of charged particles. It comprises two concentric cylindrical chambers. The inner chamber is divided into 12 symmetrical ϕ sectors, the outer chamber into 24 ϕ sectors. A single wire precision of 60 μm [50] results in a transverse momentum resolution of $\sigma(p_T)/p_T = 0.0182 \cdot p_T$ % [1].

- Z chambers situated on the outside of TEC, proportional wire chambers with a field shaped by two rings of anode wires. The proportional signals are collected in the chamber by four layers of cathode strips. Two of the layers surround the inner anode ring, two the outer anode ring. One of the two layers measures the z coordinate, the other is rotated about 20 degrees with respect to the first layer and thus provides a correlated xy and sz measurement, where $\vec{s}$ is the projection of $\vec{r}$ on the xy-plane. The z coordinate is measured with a resolution of 320 μm for Bhabha and dimuon events.

- A Silicon Micro-Vertex Detector (SMD), situated between the beam pipe and TEC. It was installed in 1993 and gives two additional high-precision space points. (More detailed information will be given in the next section).

- The Forward Tracking Chambers (FTC) situated at the forward and backward ends of TEC giving up to 4 additional space points.

The middle part of the detector is dedicated to the energy measurement of the different particles and can be divided into two parts:

- The first part is the Electromagnetic CALorimeter (ECAL) containing Bismuth Germanium Oxide ($Bi_4Ge_3O_{12}$, BGO) crystals. It has a polar angular coverage of $42^\circ - 138^\circ$ (barrel region) and 10°-35° and 145°-170° (end cap region). The energy resolution can be parametrised as [51]:

$$\frac{\sigma(E)}{E} = \sqrt{\left(\sqrt{\frac{2.37}{E}} + 0.38\right)^2 + (1.18)^2 + \left(\frac{0.25}{E}\right)^2}\ \% \tag{2.1}$$

  Besides measuring the energy, it is used for identification of photons and electrons (see section 3.6).

- The second part is the Hadronic CALorimeter (HCAL). It consists of depleted uranium absorber plates, interspersed with proportional wire chambers. The polar angular coverage is 35°-145° (barrel region) and 6°-35° and 145°-174° (end cap region). The energy resolution is given by [52]:

$$\frac{\sigma(E)}{E} = \left(\frac{55}{\sqrt{E}} + 5\right)\ \% \tag{2.2}$$

[1] This is achieved by a TEC only calibration. The use of the SMD in the TEC calibration improves the result by 6 %, see section 2.2.4

The outer part of the detector is dedicated to the measurement of muons: the MUon CHambers (MUCH). Also these are placed within the magnetic field, so they can not only be used to tag muons, but also to measure their momenta. In the MUCH a 50 GeV muon track deviates from a straight line by a sagitta of 3.4 mm over a track length of 3 m [53]. The relative precision of the muon momentum measured in the chambers is given by:

$$\frac{\sigma(p)}{p} = \frac{\sigma(t)}{t} = \left(\frac{800}{0.3} \cdot \frac{\sigma(t)}{BL^2} \cdot p\right)\% \tag{2.3}$$

where p is the momentum of the muon (in GeV), $\sigma(p)$ its error, δt the error on the sagitta t (in meters), B the magnetic field (in Tesla) and L the effective length of the track (in meters). The resolution obtained for a 50 GeV muon is $\sigma(p)/p = (2.5 \pm 0.2)\%$.

A more detailed description of all detector components can be found in [53–55]

2.2 SMD

In 1991 the radius of the beam pipe at the L3 interaction point was reduced from 8.0 cm to 5.5 cm. This allowed to enhance the tracking performance of the TEC by placing a Silicon Microvertex Detector (SMD) in the space that came free. It would, during the LEP-II period, improve the impact parameter resolution, therefore enhance the b quark tagging capability and improve the Higgs discovery potential. It was decided to install the SMD already during the LEP-I phase, so that there would be enough time for debugging in order that it run smoothly by the time LEP-II would start. Thanks to that decision it became possible to do the analysis presented in this thesis. The SMD became fully operational in 1994. The first year's (1994) running experience is described in [56]. Since the SMD is crucial for the analysis of this thesis, only data from 1994 and 1995 are used (up to the point where the LEP energy was increased to 130 GeV at the end of 1995).

2.2.1 Hardware

The SMD consists of two rings (layers) each made of 12 ladders (see figure 2.3). The inner ring is positioned at 60.7 mm from the L3 interaction point, the outer ring at 77.5 mm. Each ladder covers an azimuthal angle of ~ 30 degrees and a polar range $|\cos\theta| < 0.9$. Adjacent ladders in the inner ring have a small (5%) overlap region (see figure 2.4). Each ladder is made of 4 double-sided silicon strip detectors (called wafers). The inner side of each silicon sensor measures the z coordinate, the outer side $r\phi$. The readout strips of the outer ladders are tilted 2 degrees with respect to the inner ones, in order to minimise wrong associations of SMD hits to tracks in high multiplicity environments (see figure 2.5). The grouping of strips in the SMD readout is optimised as to reduce the number of readout channels without deteriorating the intrinsic performance. When the angle under which a track crosses a wafer changes, also the distribution of charge over neighbouring strips changes. As a consequence the accuracy of the determination of the centre-of-gravity changes. The number of strips read out is therefore reduced in the low-angle regions. The SMD also contains a radiation-monitoring system for detector safety, a cooling system, a displacement monitoring system and, of course, a mechanical support.

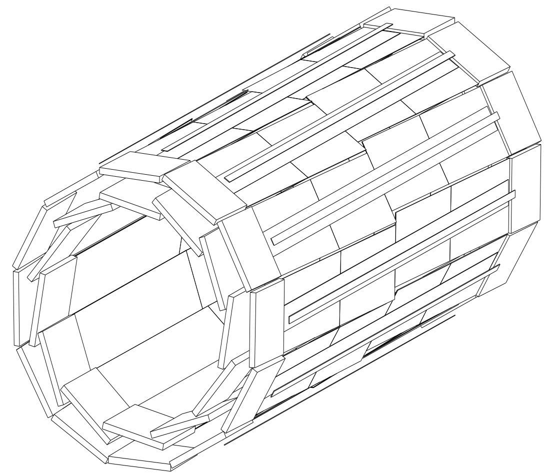

Figure 2.3: *Side view of the* SMD.

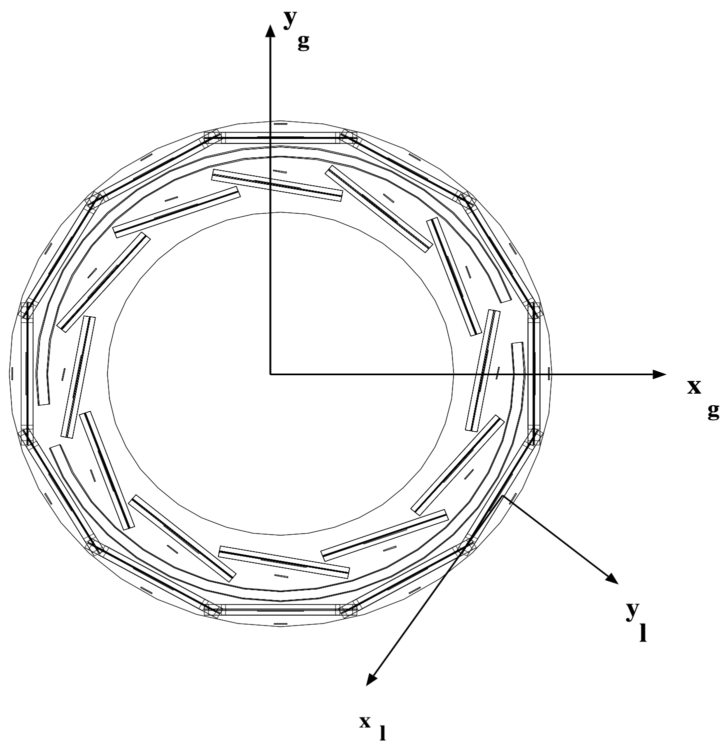

Figure 2.4: *Top view of the* SMD. *The inner ladders have a 5% overlap. Also indicated are the global (*L3*) coordinate system (x_g,y_g) and the local coordinate system of a wafer (x_l,y_l).*

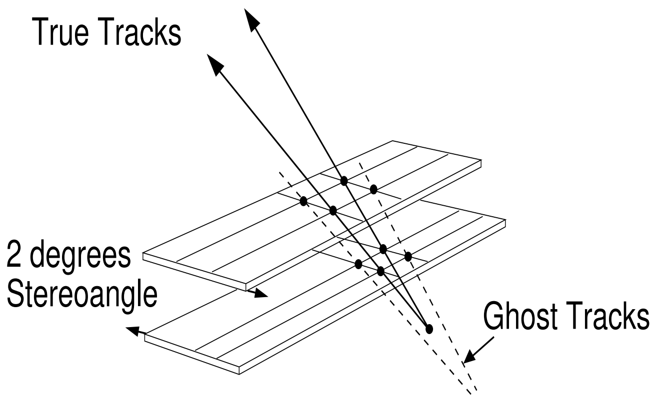

Figure 2.5: *Stereo Angle: The correct assignment of strip coordinates to a charged-particle track is aided by a 2 degree rotation (the so-called stereo angle) of the outer layer. Incorrect matches do not point back to the common vertex.*

Ladders and half-ladders

The basic unit of the SMD is the half-ladder. Each half-ladder is built of a silicon sensor pair, a kapton cable (z-side), two hybrid electronic units (in short just called the hybrid) and the structural support of the half-ladder composed of Aluminium Nitrate (AlN) and quartz plates.

Full SMD ladders are formed by joining two half-ladders with a molded carbon fibre/epoxy support rib of 300 μm thickness and an overall length of 314 mm. The rib is glued to the ϕ surface of the four silicon sensors and the surface of the hybrids. It is isolated from the ladder components by a 0.50 mm thick kapton sheet and grounded to the $r\phi$ side readout of the detector. The overall length of the full ladders is 400 mm. The metrology study in 1993 [57] measured a single ladder assembly precision of $\sim$ 5, 10 and 8 μm in the x, y, z-directions respectively, and a precision of the ladder assembly on the support structure of 15, 25 and 10 μm in x, y, z, respectively.

Sensors and Kapton cable

An SMD sensor is made of 300 μm thick high-purity n-type silicon[2] and has a surface of 70 mm by 40 mm. The junction side of the sensor carries strips implanted every 25 μm with a readout pitch of 50 μm. The strips run parallel to the long side of the sensor and measure the $r\phi$ coordinate.

[2]Impurities with 5 valence electrons have been introduced in the pure silicon that has four valence electrons. This leaves one electron for conduction. In the case of p-type silicon, the impurity has only 3 valence electrons, thus, leaving a hole behind.

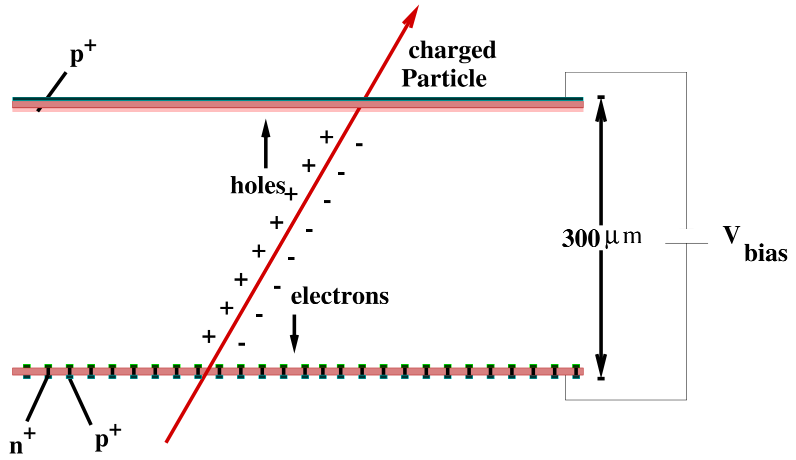

Figure 2.6: *A schematic view of the* SMD *silicon wafer.*

On the sensors ohmic side and perpendicular to the junction-side strips, n^+ strips are placed every 50 μm, with alternate p^+ strips designed to interrupt the surface charge accumulated between the n^+ strips. Since the accuracy of the determination of the centre-of-gravity changes when the track angle changes, the readout pitch is 200 μm over the polar angle θ range $0.93 > |\cos\theta| > 0.53$ and 150 μm over the range $0.53 > |\cos\theta| > 0.0$, where θ is measured with respect to the beam line. These strips measure the z coordinate. When a charged particle passes through the silicon, electron-hole pairs are created. When a voltage bias is applied across the wafer, the electrons and holes will drift to nearby strips on both surfaces (see figure 2.6).

Readout electronics and Data AcQuisition (DAQ)

In figure 2.7 a half ladder is schematically drawn. For the readout of an SMD wafer a so-called SVX chip is used. It is coupled to the Silicon sensors by a capacitor chip placed on a quartz substrate. The SVX chip is glued on an AlN substrate. This substrate is also the base of the hybrid processor. The hybrid contains surface mount resistors and capacitors for distributing chip power and sensor bias voltages and filtering. The signals from the ohmic side of a sensor (z-coordinate) are rerouted from the sensor's long edge to the readout electronics by a flexible kapton cable. This way the readout electronics on this side is taken out of the sensor's active region.

In figure 2.8 the SMD readout and data acquisition (DAQ) is drawn schematically. An intermediate electronic converter board transmits digital and analog signals between the hybrids and the external world. Analog and digital signals are sent between the SVX and the DAQ through the use of an optical transceiver board (a so-called optoboard).

The readout of the SMD silicon strips is done semi-parallel. The 48 hybrids are read out simultaneously while the strips in the 12 SVX chips of each hybrid are read out serially. The SMD signals are received at the DAQ end by a Data Reduction Processor (DRP). A DRP is a hardware filter which suppresses those signals which are not due to the passage of a charged particle through the silicon.

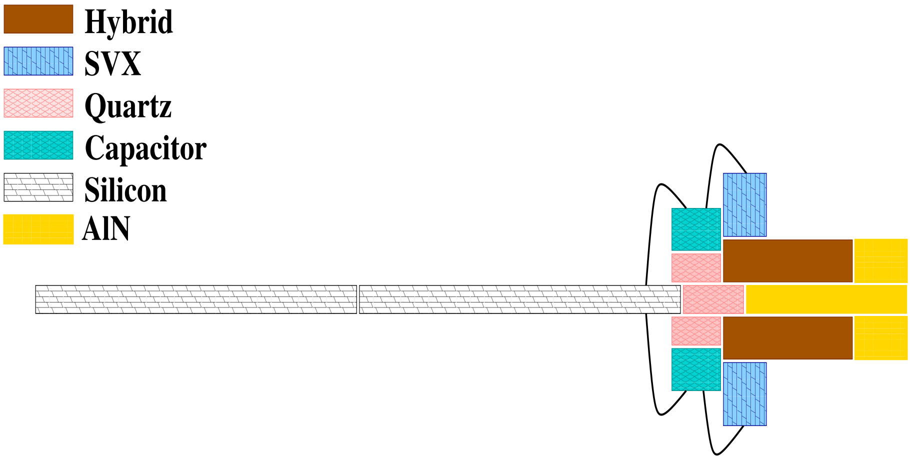

Figure 2.7: *A schematic view of an* SMD *half ladder.*

To calibrate the SMD, a run of several hundred internally generated triggers is performed to determine the Common Mode Noise (CMN)[3] for each SVX chip, along with the pedestal values (Ped) (ADC amplitude in absence of a signal) and their variance ('noise') for each SVX strip. In addition, multiple pedestals are taken with different injected test charges to determine a linear gain fit for each strip. These parameters are stored in the DRP for use by its data reduction algorithms and are also written to an external database.

Support structure

A 1m long cylindrical tube split lengthwise into 2 symmetric halves serves as the mechanical support structure for the ladders and converters of the SMD. Each half-tube is made from 3 separate carbon fibre sections. At both ends and between the sections aluminium alloy half-rings are placed. The interior half-rings contain cooling channels and provide the ladder mechanical fixation. The SMD is attached to the inner wall of the TEC with the outer two half rings.

Cooling system

The SMD components dissipate 200 W of heat. Heat instabilities may disturb the stability of the TEC drift gas. The hybrids are, therefore, cooled by a chilled water-based coolant flowing through a channel in the aluminium alloy support rings. The SMD cooling system is designed to maintain the TEC inner wall temperature at a stable working point ($18 \pm 0.1^\circ$ C) and the readout electronics temperature at some constant temperature less than about 45° C. The temperature stability of the SMD during data taking is better than 0.2°C [58].

[3]The ADC signal amplitude of all channels connected to the same wafer show a coherent time dependent shift called common noise.

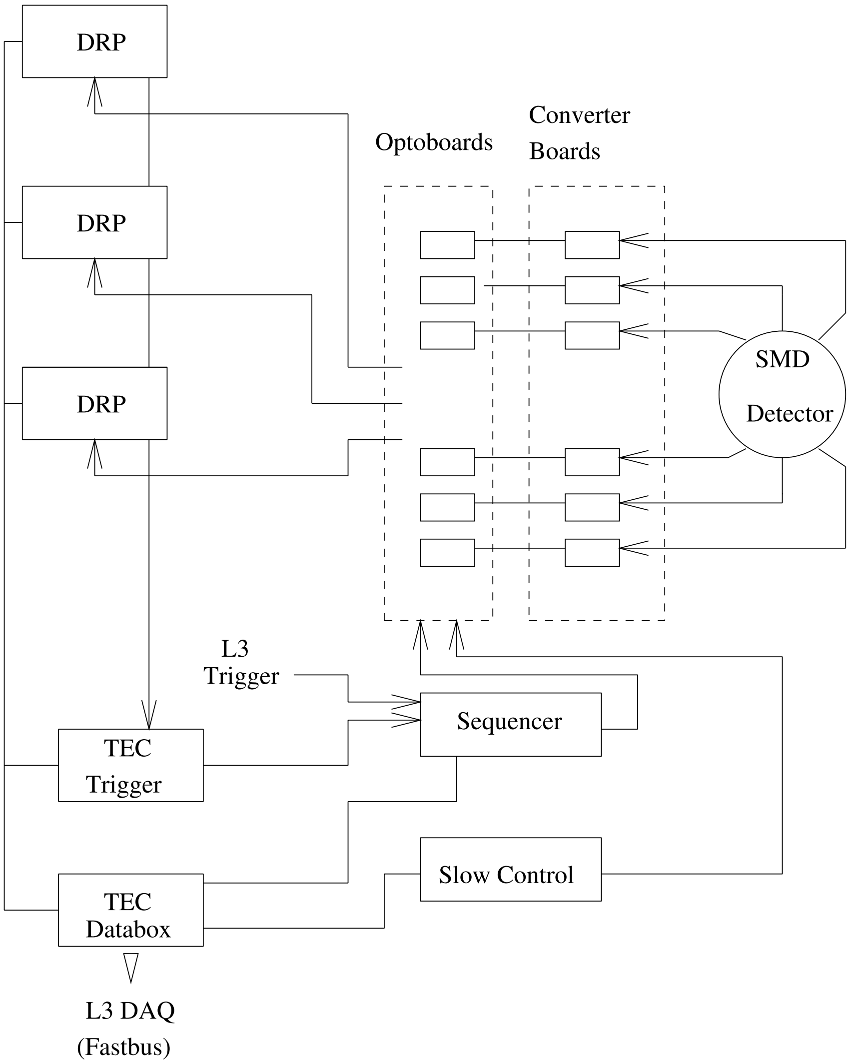

Figure 2.8: *A schematic view of the* SMD *data stream. Signals from the* SMD *detector are converted in the converter boards, 'changed' into light signals in the optoboards and sent to the DRPs. After data reduction has been performed a signal is sent to the* L3 TEC *trigger and the* L3 *DAQ.*

Radiation monitoring

A set of 12 radiation monitoring silicon diodes is installed in the vicinity of the SMD on both sides designed to measure dose rates and integrated doses and to send a beam dump signal to LEP control if the radiation dose rate in the diodes exceeds a predefined threshold. On each side there are 4 diodes. They are used for online monitoring and integrated dose calculations. Their dose rate ranges up to 70 mrad/s. Four other diodes are used for high dose rate monitoring and LEP beam dump. Their rate ranges up to 18 rad/s. Two of the diodes are used for extremely high doses. Their range is up to 6 krad/s. The two remaining diodes are left as spare diodes. The signals from the diodes are integrated over 100 μs and thus sensitive to rapid radiation fluxes. The beam is dumped if either the dose rate in the sensors on both sides of the interaction point exceeds 6 rad/s for at least 300 μs and the SMD is on or if the dose rate exceeds 600 rad/s for at least 300 μs. The latter triggers the beam dump even if SMD is off [59].

Displacement monitoring

The time dependent movement of SMD relative to the TEC is monitored by two individual systems. One system is a Laser Displacement Monitoring System (LDMS) and the other is a Capacitive Displacement Monitoring System (CDMS).

The LDMS consists of a laser diode, which produces 50 ns long pulses of infrared (λ = 905 nm) light, that is transmitted to optical heads, glued to the inner wall of TEC. Each optical head redirects the light onto the silicon wafer, striking the wafers at both 90° and 45° incidence. Test beam results [60] show that reconstruction of the centre of the light spot can be achieved to an accuracy of a few microns. A change of the centre of the light spot indicates relative translation between the SMD silicon wafer and the TEC.

The CDMS is more sensitive to angular displacements than to translations. A sensor on the SMD faces a grounded electrode on the TEC inner wall. An AC current with a frequency of 15 kHz produces a voltage drop between the sensor and the ground that is shaped to produce a nearly DC voltage which varies inversely with the capacitance of the sensor and the grounded electrode. In this way a typical sensitivity of 2.5 mV/μm is achieved for radial displacements and of 0.7 mV/μm [58] for transverse displacements. For the entire SMD six triplets of sensors are used. These triplets are positioned on the SMD support tube. Two triplets are sensitive to displacements in Δr and Δz and four triplets are sensitive to displacements in Δr and $r\Delta\phi$. The resolution, achieved under actual experimental conditions, is 1-2 μm in the radial direction and 5-10 μm in the transverse direction [58].

The running of SMD in 1994

In 1994, a significant amount of common mode noise (CMN) affected the SMD. This manifested itself in many so-called noisy channels that changed during the running period. A new calibration method was developed [56] to take into account the continuously changing noisy channels. A regular calibration was done as described in the previous part to identify the noisy channels after which the pedestals were re-computed. Therefore, the noise problem did not seriously affect the integrity of the SMD data taken during 1994. The main source of the CMN was identified to come from the (switching) power supplies of the SMD itself. A small parasitic capacitance of about 100 pF was still present causing the high CMN levels observed at the beginning of the year. The problem was fixed by synchronisation of the power supplies to each other and the LEP beam crossing [56]. In the winter shutdown, the power supplies were modified to compensate the parasitic capacitor, so in 1995 the SMD ran without CMN problems.

2.2.2 Alignment

For the alignment of the detector two coordinate systems are used. The normal/global L3 coordinate system (as defined above) and a local coordinate system for each wafer. The origin of the local coordinate system is in the centre of the active region of the wafers, the x-axis measuring the $r\phi$ coordinate, the z-axis measuring the z coordinate and the y-axis perpendicular to the sensor, going outwards with respect to the interaction point. The assumption is made that all clusters are located at y=0. See also figure 2.4.

There are two different levels of alignment. The first is the global alignment, i.e., the procedure to measure the SMD position inside the TEC. For this, the SMD is translated and rotated as a whole. Misalignment of the SMD with respect to the TEC can be corrected by three rotations around the x, y and z axes, respectively, and a translation of the SMD centre with respect to the TEC centre. A point $\vec{x_g}$ in SMD global coordinates can, therefore, be described by: $\vec{x_g} = R_z R_y R_x \vec{x_1} + \vec{x_0}$, where $\vec{x_1}$ is a coordinate vector in the ideal (i.e., misaligned) global reference system, the vector $\vec{x_0}$ is the true global position of the centre of the SMD and R_x, R_y and R_z are rotation matrices around the x, y and z axis, respectively.

After the global positioning, the individual wafers may still have a slightly different position with respect to their nominal ones and additional adjustments may be needed. The local alignment proceeds in the same way as the global alignment with rotations around the three local axes and a displacement of the centre of the wafer with respect to the nominal position. This amounts to a total of 576 (6 times 96 wafers) parameters to be determined.

In general, after the most accurate extrapolations of the TEC tracks onto the SMD wafers are found, they are compared with the actual positions of the SMD clusters. The SMD is moved to minimise the discrepancy between the two. For this exercise dimuon and Bhabha (dielectron) events are used. They have the advantage of low multiplicity, which minimises association problems between tracks and clusters.

Global alignment

To find the global alignment, one minimises the residuals of the predicted impact point of the TEC track onto an SMD wafer and the associated clusters. The χ^2 function to be minimised is the following [61]:

$$\chi^2 = \sum_{i=1}^{N_z} w_{z,i} \times (\Delta z_i)^2 + \sum_{j=1}^{N_x} w_{x,j} \times (\Delta x_j)^2, \tag{2.4}$$

where $\Delta z = z_{\mathrm{TEC}} - z_{\mathrm{SMD}}$ for clusters on the z side and $\Delta x = x_{\mathrm{TEC}} - x_{\mathrm{SMD}}$ for clusters on the the $r\phi$ side. The weights w_z and w_x are derived from the errors in the residuals in the relevant local coordinate. They are dominated by uncertainties in the TEC prediction on the wafer. The sum runs over all $r\phi$ and z clusters matched with TEC tracks.

For a more detailed description of the global alignment see reference [61]. The final results for 1994 and 1995 can be found in reference [62]. After global alignment, there is still a misalignment of the order of 20-30 μm in $r\phi$ and 50-100 μm in z [61].

Local alignment

The predictions of TEC-only tracks on the SMD wafer are not precise enough for the purpose of local alignment. The prediction can be improved by adding another SMD cluster to the TEC track. There are two possibilities: (same) side prediction and back-to-back prediction. For the side prediction, the SMD cluster under consideration is compared to a track that has been refitted with either an SMD cluster in the other SMD ring, or a cluster in the overlapping ladder, or a combination of the two (see figure 2.9). The overlap region provides information on relative positions inside the ring. The comparison of hits in the inner and outer ring provides information on the relative position of the two rings.

For the back-to-back prediction dimuon and Bhabha events are selected. Here, a wafer on one side of the SMD is positioned with respect to a wafer on the opposite side of the SMD. In the case of the L3 detector with a magnetic field of 0.5 T and a silicon detector very close to the vertex, the assumption is made that all hits lie along a straight line. This increases statistics since predictions can be made with only two SMD points.

The χ^2 to be minimised is the same as that for the global alignment given in eq. (2.4), but the differences are in local coordinates and the predictions come either from the side- or the back-to-back case or both. Both x_{SMD} and z_{SMD} hits are required on a wafer unless one side of the wafer is known to be non- or badly functioning. Alignment parameters are determined assuming they are small, so only first-order terms are taken into account. In the aligned system, new predictions are obtained and the alignment procedure is iterated until individual residues reach 0.1 times the estimated error or the χ^2 value begins to increase. The results can be found in [62].

2.2.3 Track Matching

The outer layer of the SMD is rotated 2° with respect to the inner layer around the axis perpendicular to its wafer plane. This rotation correlates the xy and z measurements.

The measurements in the local SMD reference system l_i $(i = 1,4)$ [4] can be rotated and translated to L3 global coordinates in the two rings A (inner) and B (outer) in the following way:

$$\begin{aligned}
\mathrm{A}: \quad & x_a = l_2 && \text{Layer } 2 && (2.5)\\
& y_a = 0 && && (2.6)\\
& z_a = l_1 && \text{Layer } 1 && (2.7)\\
\mathrm{B}: \quad & x_b = l_3 \sin\theta + l_4 \cos\theta && \text{Layer } 4 && (2.8)\\
& y_b = 0 && && (2.9)\\
& z_b = l_3 \cos\theta - l_4 \sin\theta && \text{Layer } 3, && (2.10)
\end{aligned}$$

where $\theta \simeq 2^\circ$ is the 'stereo angle' of the outer layer.

For the matching only well-measured TEC tracks and SMD clusters are used. The TEC tracks must satisfy the requirements:

- DCA < 80 mm.

[4] l_1 (l_2) represents a hit in the inner SMD z (ϕ) layer z_{inner} (ϕ_{inner}) and l_3 (l_4) represents a hit in the outer SMD z (ϕ) layer z_{inner} (ϕ_{outer}).

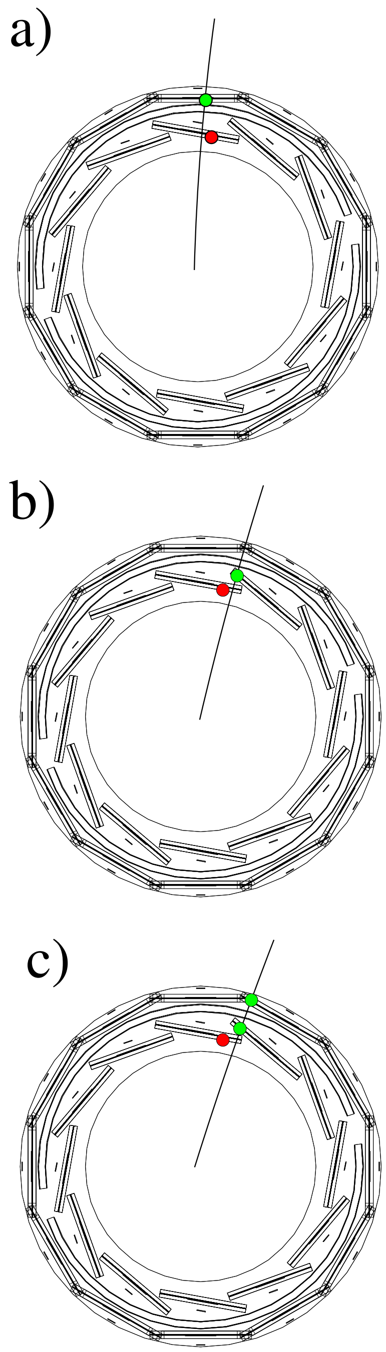

Figure 2.9: *Types of 'side' predictions for the internal* SMD *alignment. a) Two layers, b) overlap, c) best case.*

- number of TEC hits ≥ 10
- span ≥ 15
- sz fit performed,

where, the DCA is the distance-of-closest-approach in the transverse plane to the interaction point, and the span is the length of the track expressed as the number of wire distances covered in TEC.

An SMD cluster consists of a group of SMD strips that were hit, i.e. strips were upon charge is deposited by a particle that passes through the SMD wafer. The SMD clusters are selected by the following criteria:

- cluster amplitude ≤ 250 ADC counts
- number of cluster hits ≥ 1
- signal/noise ratio of cluster ≥ 5
- cluster width(number of strips) $\geq \begin{cases} 3 & \text{for } x \text{ clusters,} \\ 5 & \text{for } z \text{ clusters.} \end{cases}$

A track is extrapolated to the ladder under consideration. In layer 2, simply, the cluster closest to the prediction within 3.5 times the uncertainty is taken. If two different tracks point to the same cluster, the cluster is associated to the closer track in layer 2. Due to the overlap region it is possible that one track has two clusters associated with it. These clusters are in different ladders, however. With an ideal MC sample, i.e., without detector effects taken into account, an efficiency to find at least one hit on a track that crosses layer 2 of $(88.2 \pm 0.3)\%$ is obtained. A misidentification rate was found to be $(1.0 \pm 0.1)\%$ [63].

Layer 4 only contributes to an improvement of the TEC track if also a cluster in layer 3 is found (because of the stereo angle). It is, therefore, decided to take just the closest cluster in layer 4. The resulting efficiency is (76.7 ± 1.1) % on tracks with an associated cluster in Layer 2 and the misidentification rate is $(1.1 \pm 0.3)\%$ [63].

For association in Layer 3 an improved prediction, the so-called 'stereo-prediction', is used. From eq. (2.8) follows:

$$l_3^{\text{predicted}} = \frac{x - l_4 \cos\theta}{\sin\theta}, \tag{2.11}$$

where x is the global coordinate in the xy plane (from the TEC) and l_4 is the local cluster prediction. Using all events with a cluster in the 4th layer and taking the cluster in layer 3 closest to the stereo prediction, an efficiency of $(91.8 \pm 0.2)\%$ is obtained. The misidentification was found to be $(2.7 \pm 0.2)\%$ [63].

After the track is refitted with the 'stereo' clusters found in the outer layers, the residues of the TEC prediction and clusters in layer 1 are taken. There are long tails in the distribution that come from tracks not pointing to the interaction vertex. These residues are improved if a better estimate of the z-coordinate of the event vertex is found and the tracks are refitted with this improved vertex constraint. However, tails remain since not all tracks (for instance b-decay tracks) originate from the vertex. With the improved prediction an efficiency of $(84.7 \pm 0.3)\%$ is obtained, with a misidentification rate of $(4.2 \pm 0.2)\%$ [63]. Finally, all clusters closest to the track after all previous refits are accepted.

2.2.4 Calibration of TEC with SMD

A further advantage of the SMD is that now the calibration of the TEC can be improved with information from the SMD. Instead of performing the TEC calibration with information mainly coming from the chamber itself (an iterative and difficult procedure) it can be done using mainly information from outside TEC and is non-iterative, stable and can reach the internal precision of the chamber. This way, the TEC resolution improves [64](for the 94b period):

- the angular resolution from 0.9 to 0.4 mrad,
- the DCA resolution from 133 to 105 μm,
- the p_T resolution from 0.0182 to $0.0171 \cdot p_\mathrm{T}$ %.

2.2.5 SMD efficiency

Experimentally, not all tracks are matched with hits in all four layers of the SMD. This inefficiency can have several causes:

- digitiser and amplifier (the hybrid) malfunction (dead half ladder)
- noisy channels
- a dead z_outer layer causing also a dead ϕ_outer layer
- wrong TEC prediction
- aging effects

The ladder efficiency ε_l, defined as the number of times a cluster is associated with a track that crosses the active region of the ladder. For both SMD inner layers and the z_outer layers efficiencies are found of about 80 to 85 % and for the ϕ_outer layers an efficiency of about 65 % [65]. This last lower efficiency is due to the fact that a coincidence is required with a z_outer hit.

2.2.6 SMD resolutions

The SMD point resolution is 10 μm in the $r\phi$ plane and 21 μm $\oplus$ 15 μm / $\tan\theta$ and 21 μm $\oplus$ 26 μm / $\tan\theta$ in the sz plane for the normal and large pitch region, respectively. The symbol $\oplus$ indicates that the numbers should be added in quadrature. Thus a vertical track has a resolution of 21 μm in the sz plane.

Another important measure of physical precision is the distance-of-closest-approach resolution. With the SMD a DCA resolution of 66 μm is obtained in hadronic events (see figure 2.10).

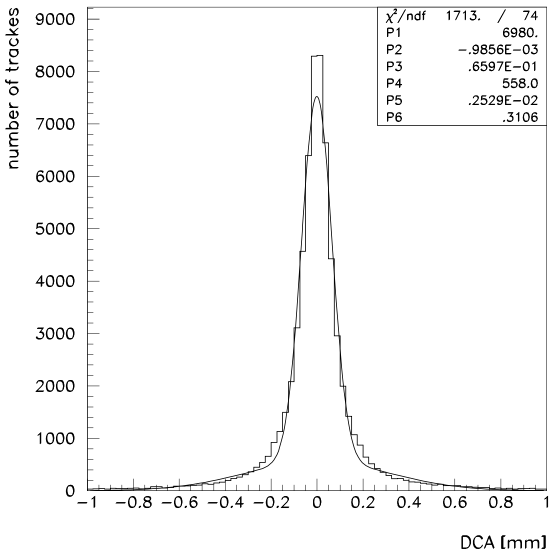

Figure 2.10: *The DCA resolution in hadronic events. For the fit a double Gaussian is used. P1 and P4 are the heights of the two Gaussians, P2 and P5 are the mean values and P3 and P6 are the widths.*

2.3 The simulation

To study the efficiencies and purities of the collected data, they are compared with Monte Carlo (MC) simulated data. This simulation is performed in two stages. First, the events are generated according to our present knowledge of particle production in the reactions:
$e^+e^- \rightarrow \gamma/Z \rightarrow q\bar{q} \rightarrow$final state particles. The program used to describe these reactions is JETSET [66]. After that, the detector simulation is run. Two specific software packages are used: GEANT [67] and SIL3 (SImulation of L3). The first package is very general and can be used to simulate the interaction of any particle with any detector material, the second package is L3 specific. The simulated events are written to tape in the same format as are normal data events.

The inefficiency of the detector subcomponents is taken into account by the software from information of a database containing the sub-detector performances during actual data taking runs. A MC run with a fully operational detector is called ‘ideal’ detector MC simulation. When time dependent effects are taken into account, the MC simulation is called a ‘real’ detector simulation.